Available online at www.sciencedirect.com

ScienceDirect

Transportation Research Procedia 3 (2014) 339 – 348

Transportation Research Procedia

www.elsevier.com/locate/procedia

17th Meeting of the EURO Working Group on Transportation, EWGT2014, 2-4 July 2014, Sevilla, Spain

Estimating Travel Time Distribution Under Different Traffic Conditions

Younes Guessous[a], Maurice Aron[b], Neila Bhouri[b], Simon Cohen[b]

[a] *Ecole des Ponts-ParisTech, 6-8 avenue Blaise Pascal, Cité Descartes 77455 Champs sur Marne Cedex, France*
[b] *IFSTTAR/COSYS/GRETTIA, 14-20 bd Newton 77447 Champs sur Marne Cedex, France*

Abstract

Increasing mobility and congestion results in an increase in travel time variability and in a decrease in reliability. Reliability becomes an important performance measure for transportation facilities. A variety of performance measures have been proposed to quantify it. Many of these indicators are based on percentiles of travel time. The knowledge of the distribution of travel time is needed to properly estimate these values. Congestion distorts the distribution and particular statistical distributions are needed. Different distributions have been proposed in the literature. In a previous paper, we presented a comparison of six statistical distributions used to model travel time. These six distributions are the Lognormal, Gamma, Burr (extended by Singh-Maddala), Weibull, a mixture of two Normal distributions and a mixture of two Gamma distributions.
In this paper a probabilistic modeling of travel time which takes into account the levels-of-service is given. Levels of service are identified, then travel time distributions are modeled by level of service. This results in a very good fit between the empirical and modeled distributions Moreover, the adjustment was improved, thanks to the calibration of "Bureau of Public Roads" functions, linking the travel time to the traffic flow by level of service.
The superiority of the Singh-Maddala distribution appears in many cases. This has been validated, thanks to travel time data from the same site at another period. However the parameters of the distributions vary from one year to another, due to changes in infrastructure. The transferability of the approach, not performed, will be based on travel time data on another site.

Selection and peer-review under responsibility of the Scientific Committee of EWGT2014

Keywords: congestion; traffic flow; travel time; motorway; modeling; statistics; reliability; distribution; Level of Service; Bureau of Public Roads.

1. Introduction

Traffic congestion impacts speed, thus travel time. When traffic increases and approaches the full capacity of the network, the flow becomes unstable and much more vulnerable to incidents, road works or bad weather. This

2352-1465
Selection and peer-review under responsibility of the Scientific Committee of EWGT2014
doi:10.1016/j.trpro.2014.10.014

increases the variability of travel time, to which users are very sensitive. Therefore, travel time reliability has become an important performance criterion for transportation facilities, complementing the traditional measures such as delay and average travel time. In recent research, a variety of performance measures have been proposed to quantify reliability and monetize it. This includes planning time, buffer time, standard deviation, coefficient of variation, skewness,... - an overview is given in Lomax et al. (2003). These indicators are based on percentiles of travel time. The knowledge of the travel time distribution is then needed.

Different distributions are presented in the literature as the best way to model the travel time distribution. Richardson and Taylor (1978), Rakha et al., (2006), Pu (2010) and Arezoumandi (2011) concluded for a Lognormal distribution. Polus (1979) concluded for a Gamma distribution; however Al-Deek and Eman (2006) proposed a Weibull one. Taylor and Susilawati (2012) and Susilawati et al. (2012) adopted the Burr XII distribution; the advantage of this latter method is that its tails often fits the empirical ones. Aron et al. (2012) presented a comparison of six statistical distributions used to model travel time. The parameters of these distributions have been identified on the basis of real time data collected on a weaving section of the A4-A86 French urban motorway.

Based on the same data, this paper uses the Burr XII distribution, completed by a scale parameter introduced by Singh and Maddala (1976) to model travel time over five levels of service. The next section is dedicated to data collection. A method for levels-of-service extraction using the fundamental diagram is given in section 3. Calculation of the travel time and modeling of its distribution over five levels-of-service are presented in section 4. In section 5, the travel time distribution calibration is improved, using relations linking travel time to flow.

2. Data collection

The data used in this paper was collected on a weaving section of the A4-A86 French urban motorway. A two-lane urban motorway ring (A86) round Paris and a three-lane West-East urban motorway (A4) meet in the east of Paris and share a four-lane 2.3 km-long section. Traffic is particularly dense at some hours, and causes the greatest traffic bottleneck in Europe. Data used in this paper were collected in the year 2002 and 2006, on a 3-km long stretch (2.3 on the weaving section, 0.7 km downstream), in the Eastbound direction. 133,000 and 131,000 vehicles circulate by day on the weaving section in 2002 and 2006. Four inductive loops (three on the weaving section, one downstream) provide every six minutes flow, occupancy and average speed by lane.
Table 1 provides the average speed, after weighting by the six-minute traffic flow, in 2002 and 2006.

Table 1 Average six-minute flow and average speed (in km./h) by lane and section

Year	2002				2006			
Station\Lane	Lane 1	Lane 2	Lane 3	Lane 4	Lane 1	Lane 2	Lane 3	Lane 4
Station 1	55	54	62	68	66	68	74	75
Station 2	53	64	83	92	67	79	87	96
Station3	44	56	69	73	66	77	87	92
Downstream	78	77	97	108	118	101	108	117

Note than in 2006, a Hard Shoulder Running (HSR) experiment consisted in opening the hard shoulder to vehicles when traffic density was high - Bhouri and Aron (2014). The average speed on this lane is not given here.

Although the data are generally very good, some are missing, inaccurate or irrelevant. A mean speed for one lane lower than 2 km/h or higher than 150 km/h, is considered as an outlier. Other anomalies in traffic data are identified – occupancy greater than 100% or 6-minute flow (by lane) greater than 400 vehicles. In these cases the data for the corresponding period and lane are cancelled and considered as missing. When this occurs in 2002, the missing data for a given period and lane is substituted, when possible, by data from a corresponding period from the year 2001 or 2000, the same day of the week, the same exact time and approximately the same date.

Although there are 24*365=8,760 hours a year, or 87,600 6-minute periods, only 53,646 periods are considered here because data are “good” for a period only when all the four inductive loop are “good” in 2002 and 2006.

3. Travel Time and Level-Of-Service

3.1. Travel Time estimation

There are different methods available to calculate the travel time from loop detector data, such as extrapolation of the point speed values, statistical methods, and models based on traffic flow theory. Here the travel time is obtained by as extrapolation of the point speed values of the loop detector data aggregated on six-minute periods. But:

According to Nam & Drew (1999), biases occur for certain traffic conditions. Vanajakshi et al. (2009) developed, thanks to the traffic flow theory, a method able to improve travel time for all traffic conditions (normal flow, transition to congestion, congestion). This method is not considered here because data processing alters distributions.

- Aggregated speeds are used and it is not possible to properly derive individual velocities from aggregated ones. Indeed, let $V_d(x)$ be the instant speed of driver *d* at a point *x* of the section of length *L*. His travel time for the section is $\int_0^L dx \,/\, V_d(x) = L/V_{h,d}$ where $V_{h,d}$ is the harmonic speed average of driver *d* on the section. $V_{h,d}$ is generally not equal to V_d, the speed of driver *d* on the sensor downstream. The average travel time for the *Q* drivers exiting the section is $1/Q \sum_{i=1,Q} \left(L/\,V_{h,i}\right) = L/\,V_h$, where V_h is the harmonic average speed (on all drivers). However, assuming that, for all drivers d, the instant speed V_d at the end of the section is equal to V_{hd}, implies that $V_h = V$, (*V* being the speed given by the detector, which is the harmonic average of the $\{V_d\}$. With this assumption only, the loop detector travel time is correct.
- Even if the travel times obtained with aggregated speeds were perfectly equal to the average of individual travel times, the distributions and meanings of aggregated and individual travel times are different. Fortunately the aggregated travel time distribution is in certain cases preferable to the individual one: a driver, wanting to leave or arrive in a particular time interval, prefers having an information or prediction on the aggregated distribution on a (six-minute) period. He will modify such information as he considers himself a slow or fast driver.

3.2. Fundamental Diagram

In the following, the traffic flow, density and average speed are noted *q, k,v,* with the indices *i* (i=1,n) for the lane and *j* (j=1,m) for the section. The equivalent flow, density and average speed for the set of the *n* lanes and *m* sections have no index. The three macroscopic traffic variables are linked by the equation $q=k.v$. The Fundamental Diagram, based on a decreasing relation between speed and density, models the flow-density relationship. An example of a fundamental diagram, plotted on the basis of experimental data is provided in Figure 1. The first part of the graph represents the free flow, where the interaction between vehicles is light; then traffic flow increases along with traffic density until the critical density value k_c. Corresponding flow is the maximal flow q_{max} sustained by the infrastructure. Above this density, vehicles are bunched and flow decreases.

3.3. Construction of a fundamental diagram for consecutive sections

Aggregation of data over lanes in one section is obtained by applying simple operations to the three traffic variables. We add traffic flows to obtain the flow for an entire section and we similarly add traffic densities. Speed for the entire section is the result of dividing the flow by the density. Formulas are the following:

$$q_j = \sum_{i=1}^{n} q_{ij} \;\; ; \;\; k_{ij} = \frac{q_{ij}}{v_{ij}} \quad \text{or} \quad \frac{1}{v_{ij}} = \frac{k_{ij}}{q_{ij}} \; ; k_j = \sum_{i=1}^{n} k_{ij} \;\; ; \frac{1}{v_j} = \sum_{i=1}^{n} \left(\frac{k_{ij}}{q_{ij}}\right) \cdot q_{ij} \Big/ \sum_{i=1}^{n} q_{ij} = \frac{k_j}{q_j} \tag{1}$$

The last equation gives the harmonic average speed, weighted by traffic flows. Let L_j be the length of section j, thus L_j/v_j is its travel time. Travel times on consecutive sections being additive, the equation of the global average speed and of the equivalent density on consecutive sections, are:

$v = \sum_{j=1}^{m} L_j / \sum_{j=1}^{m} \frac{L_j}{v_j}$ (2); as $N = \sum_{j=1}^{m} L_j \cdot k_j$ vehicles are present on the sections: $k = \sum_{j=1}^{m} L_j \cdot k_j / \sum_{j=1}^{m} L_j$ (3)

The flow is then the average of sections' flows weighted by travel times. It is also the total travel time (for all users) divided by the average travel time.

The global fundamental diagrams in 2002 and 2006 are shown in Figure 1(a) and 1(b). In 2006 points become less dense around 160 vehicles/km, whereas in 2002 they do so around 180 vehicles/km. That can be interpreted as the positive effect of opening hard shoulders to vehicles when congestion exceeds a certain level.

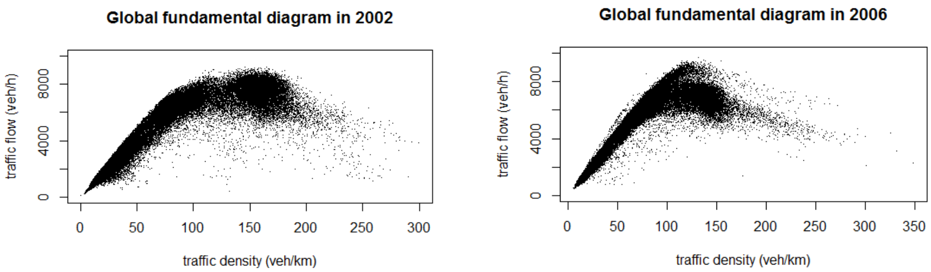

Figure 1 (a) Global fundamental diagram in 2002 (b) Global fundamental diagram in 2006 direction Paris to the East

3.3 Fitting the fundamental diagram

The levels of services are defined with respect to road capacity and critical density. Road capacity is not assumed to be the maximum observed traffic flow, which could be an outlier. Here road capacity is determined after fitting, in a first step an analytic curve to the scatter plot; the maximum of this curve gives the capacity. Numerous models are used to fit the fundamental diagram. Some are summarized in Table 2.

Table 2. Statistical models for fundamental diagrams

Model	Equation
Greenshields	$q=a*k+b*k^2$
Generalized power	$q=a*k+b*k^\alpha$
Underwood	$q=a*k*\exp(-b*k)$
Generalized exponential	$q=a*k*\exp(-b*k^\alpha)$

For each model we apply a nonlinear regression analysis, based on the least-square method. All computations in this article are performed using R statistical free software statistical language. Details about the software and its features can be found in Heiberger and Holland (2004).

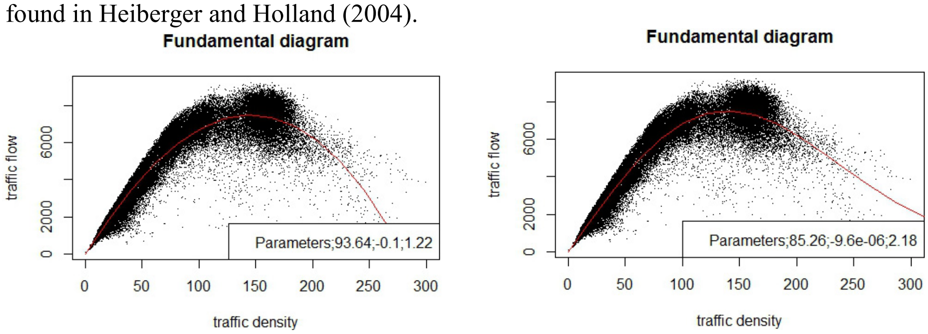

Figure 2. Global fundamental diagram in 2002 fitted with (a) a generalized power model (b) a generalized exponential model Number of data: 53677; Residual standard error for (a) : 707.4 ; for (b) : 696.5

We compared only the generalized models. Figure 2 above and Figure 3 below show the adjustments of the generalized power and exponential models on the global fundamental diagram in 2002 and 2006.

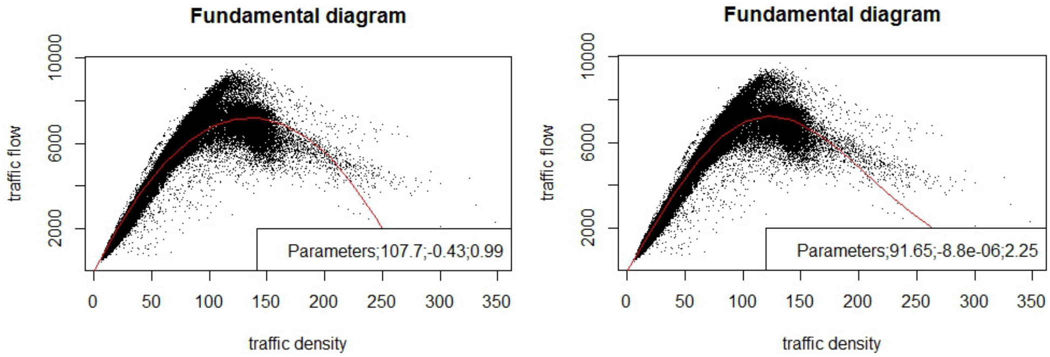

Figure 3. Global fundamental diagram in 2006 fitted with (a) a generalized power model (b) a generalized exponential model; Number of data: 53677; Residual standard error for (a) : 655; for (b) : 588.2

The Generalized Exponential, giving the best representation of the scatter plot's tail, is selected here.

3.4 Level-of-service computation

The road capacity and the critical density appear on the fitted fundamental diagram; separating the diagram in levels of service (LOS) is straightforward, using the LOS thresholds in terms of capacity percentage and density. The six LOS defined by the High Capacity Manual are here replaced by five LOS, defined as following:

Table 3: Definition of LOS

	LOS 1	LOS 2	LOS 3	LOS 4	LOS 5
Flow	< 75%capacity	between 75% and 90% of capacity	> 90%capacity	> 90%capacity	< 90% capacity
Density	< critical density	< critical density	< critical density	> critical density	> critical density

Four points separate the five LOS. Point A (between LOS 1 and 2); B (between LOS 2 and 3); C (between LOS 3 and 4); and point D (between LOS 4 and 5). Their flow, density and speed are given in Table 4.

Table 4. Flow, density and speed at four points separating the five LOS for 2002 and 2006

	2002			2006		
Points	Flow	Density	Speed	Flow	Density	Speed
A	5628.2	74.1	75.9	5414.3	65.9	82.1
B	6753.8	98.0	68.9	6497.2	86.9	74.7
C	7504.2	139.2	53.9	7219.1	122.8	58.8
D	6753.8	184.0	36.7	6497.2	161.6	40.2

4. Modeling travel time distribution by Level-Of-Service

Figure 4(a) and 4(b) show the placing of the five LOS and of the four separating points. Furthermore, in Figure 5 are displayed the travel time histograms by LOS; these are useful to select the distributions required for modeling.

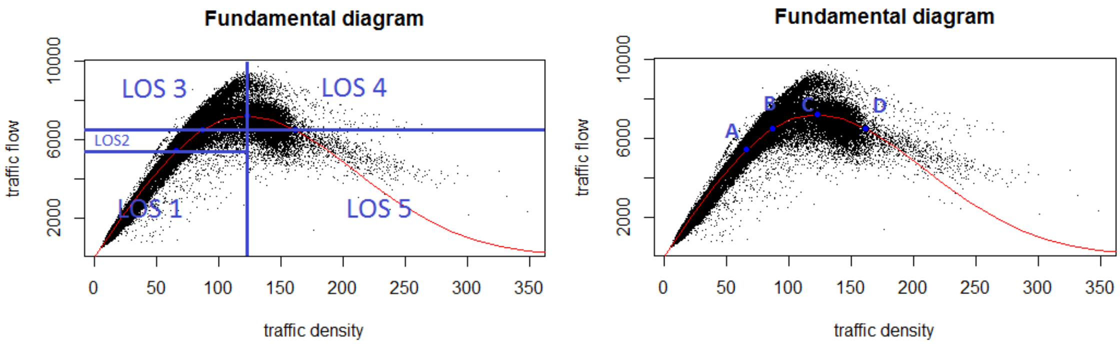

Figure 4. (a) Levels-of-service selection (b) Points separating the LOS

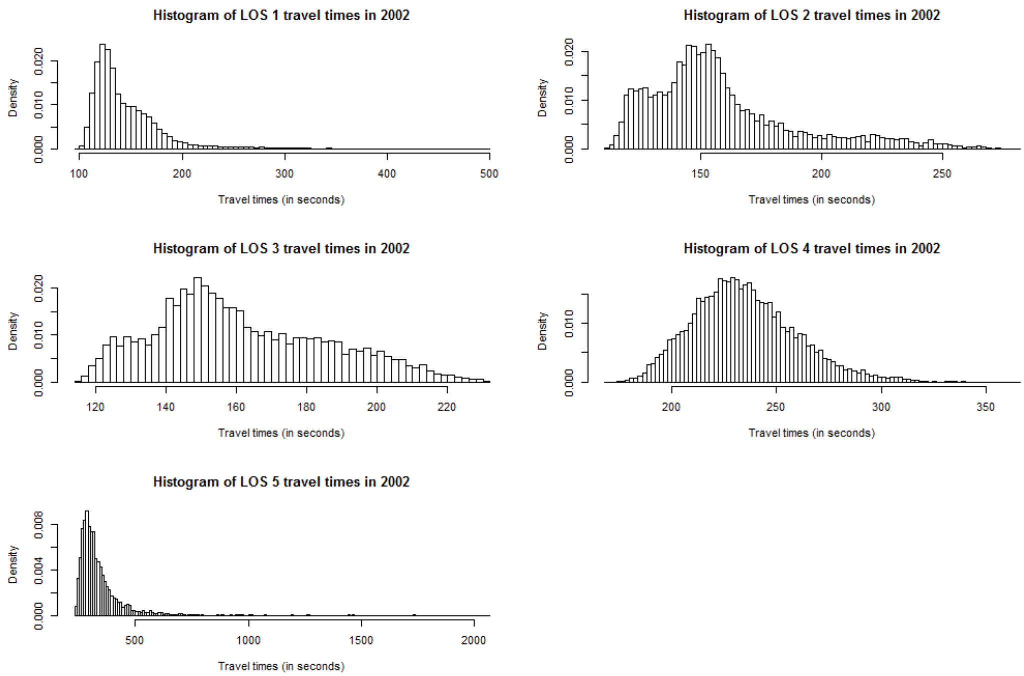

Figure 5. Histogram of travel times separated by LOS in 2002

The likelihoods of the lognormal and Singh-Maddala distributions are maximized on each LOS histogram. The cumulative density function F(x) and the probability density function f(x) of the Singh-Maddala distribution are given below; any Singh-Maddala percentile P(α) of range α (α between 0% and 100%) derived by inverting F(x);

$$\text{For } x>0\text{: } F(x)=1-[1+(x/b)^{a}]^{-q} \quad ; f(x)=a\cdot(q/b)\cdot[1+(x/b)^{a-1}]^{-q+1} \; ; \quad P(\alpha)=b\cdot\sqrt[a]{(1-\alpha)^{-1/q}-1} \tag{4}$$

The 1st and 3rd parameters, a and q are shape parameters, whereas the second parameter b is a scale parameter.

For the first three LOS, a normal mixture model is also fitted. We evaluate the quality of the models by using the Akaike information criterion (AIC), and select the model that minimizes this criterion (Table 5).

Table 5. AIC for the five LOS and three distribution models in 2002 (best distribution highlighted)

LOS	Number of data	Singh-Maddala	Lognormal	Normal mixture
1	24036	221876.36	230326.73	227150.70 (with 2 components)
2	7878	73971.82	74746.84	73530.72 (with 2 components)
3	6599	60821.46	60512.36	59872.96 (with 3 components)
4	10989	101480.51	101325.77	Not performed
5	4144	46622.16	49089.62	Not performed

When identifying the best parameters for a model by the likelihood maximum method, the Akaike information criterion (AIC) is derived; it is equal to 2k-2ln(L), where k is the number of parameters of the model and L the likelihood maximum; AIC is a measure of the relative quality of a statistical model for a given set of data. The computations of AICs for different models result in selecting the best one (the one with the minimum AIC). However, even this best one can be rejected (against a null hypothesis) if its p-value (not given here) is less than a given threshold (5% for instance). Burnham and Anderson (2004) have established that this criterion is better than BIC (Bayesian Information Criterion), using theoretical arguments and simulation studies.

LOS 3, 4 and 5, are the most interesting ones, because they occur near capacity or in congestion. Their adjustments to the models are presented here. Adjustments with a normal mixture have not been performed for LOS 4 and 5 because the empirical histograms have a single mode.

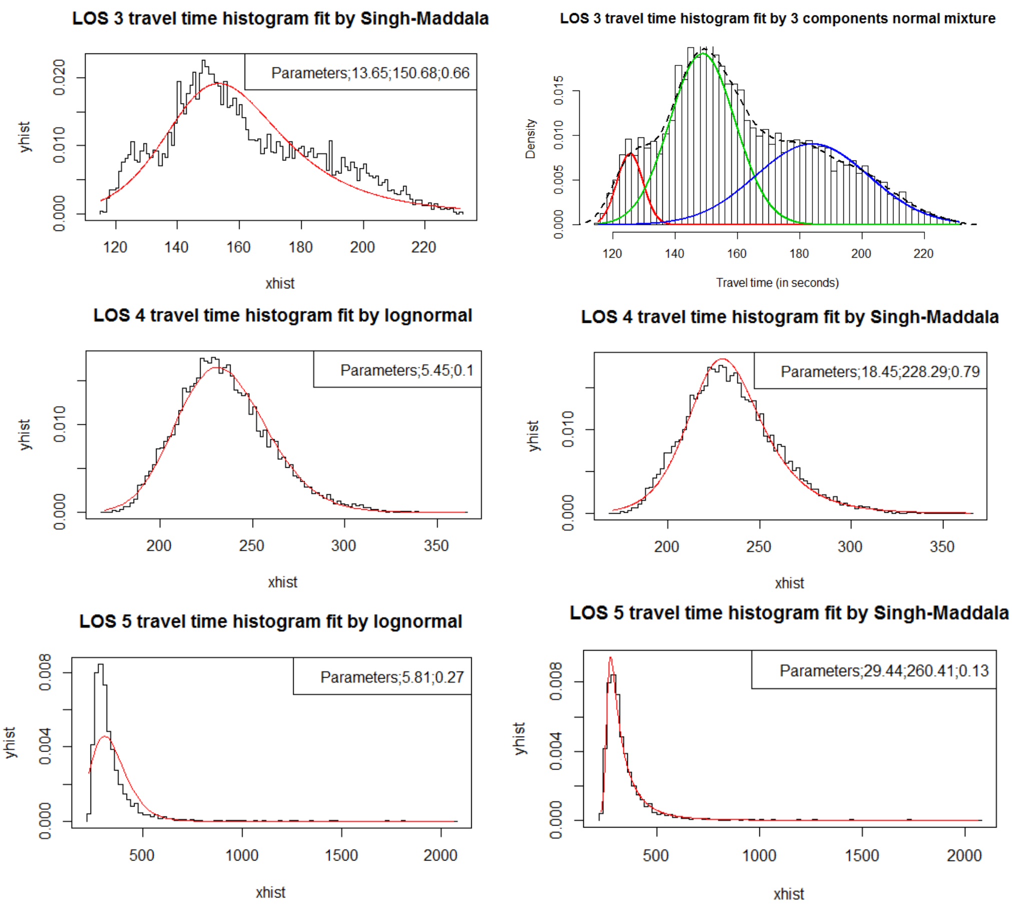

Figure 6. Histograms of LOS 3, 4 and 5 travel times fitted by different distributions in 2002

For LOS 3, three modes appear, and a three-component normal mixture outperforms Singh-Maddala.

For LOS 4, the AIC for the lognormal distribution is better than the one for the Singh-Maddala. However, the difference in this criterion between lognormal and Singh-Maddala is not significant enough, compared to the same difference in LOS 3. Besides, we do not notice any significant difference graphically.

For LOS 5, Singh-Maddala outperforms the lognormal distribution from the AIC and graphics points of view.

With the AIC, the superiority of the Singh-Maddala distribution is confirmed from 2006 data for LOS 1, 4, 5, whereas it is lightly outperformed by normal mixture in LOS 2 and 3 (Table 6). The lognormal distribution lags far behind Singh-Maddala and normal mixture, except for LOS 4 where it is close to Singh-Maddala.

Table 6. Akaike information criterion for the five LOS and three distribution models in 2006

LOS	Number of data	Singh-Maddala	Lognormal	Normal mixture
1	23816	165571.60	178098.76	166346.62 (with 2 components)
2	9508	73814.98	78407.83	73757.59 (with 2 components)
3	10306	79115.66	82729.76	78913.22 (with 2 components)
4	6248	56111.66	56284.97	Not performed
5	3760	39100.80	40434.25	Not performed

Table 7 provides estimates for Singh-Maddala parameters in 2002 (and in parenthesis for 2006, LOS 1 only).

Table 7. Estimates and 95% confidence intervals for Singh-Maddala parameters (five LOS in 2002 and LOS 1 in 2006)

LOS	Parameter	Lower bound	Estimate	Upper bound
	shape1.a	31.98 [47.87]	32.01 [47.90]	32.05[47.92]
1	Scale (in seconds)	115.65 [108.63]	115.65 [108.63]	115.65 [108.63]
	Shape 3 *q*	0.11 [0.27]	0.15 [0.31]	0.19 [0.34]
	shape1.a	16.49	16.53	16.57
2	Scale (in seconds)	136.31	136.32	136.33
	Shape 3 *q*	0.31	0.38	0.44
	shape1.a	13.61	13.65	13.69
3	Scale (in seconds)	150.67	150.68	150.69
	Shape 3 *q*	0.58	0.66	0.74
	shape1.a	18.42	18.45	18.48
4	Scale (in seconds)	228.28	228.29	228.29
	Shape 3 *q*	0.73	0.79	0.85
	shape1.a	29.35	29.44	29.52
5	Scale (in seconds)	260.40	260.41	260.42
	Shape 3 *q*	0.03	0.13	24

Let us recall that Singh-Maddala distribution has 3 parameters, while a normal mixture with 2 components has 2×2=4 parameters. We recommend using Singh-Maddala distribution: it is the most stable distribution and adapts to various levels-of-service. It provides a good trade-off between fitting quality and model simplicity. The numerical values obtained for the Singh-Maddala parameters differ between years 2002 and 2006 (same periods in the year); the 2002 values are given in the brackets (only for LOS 1) in the preceding table: 2006 values (given in Table 7 for the first LOS) differ from 2002 values -. This is probably due to a better compliance in the speed limit, after an enforcement campaign launched in 2003, and to the HSR experiment in 2006.

5. Improving travel time models

One way to improve travel time prediction is to find a relationship between travel time and flow. The maximum flow (capacity) is one of the key parameters of such relationships The most widely used capacity restraint function was determined by the Bureau of Public Roads (BPR) in the USA. Here this function is applied by LOS:

$$T_\ell = T_0\left(1+\alpha\cdot\left(\frac{q_\ell}{q_{\max}}\right)^\beta\right) \quad (5)$$

where T_0 is the travel time when there is no traffic; T_ℓ (ℓ =1..5) the travel time for LOS number ℓ, . α and β are dimensionless parameters; thanks to the non-linear regression package of the R software, their values and the quality of the regressions (the p-value and residual standard error) have been obtained and are presented in Table 8.

Table 8. Statistical information for the five LOS in 2002

LOS	Number of data	Residual standard error (seconds)	α		β	
			Estimate	p-value	Estimate	p-value
1	24036	76.61	1.419	<2e-16	0.454	<2e-16
2	7878	30.46	0.871	<2e-16	0.005	0.87
3	6599	24.32	0.926	<2e-16	0.135	7.06e-05
4	10989	24.21	1.750	<2e-16	-0.255	<2e-16
5	4144	139.4	2.606	<2e-16	-0.832	<2e-16

As p-values are below 0.05 (except for LOS 2), the BPR functions, relating travel time and traffic flow are significant for LOS 1, 3, 4 and 5. Residual standard errors are generally acceptable (see Table 8), given the facts that in free-flow (LOS 1) the speed is not constrained by the flow, and that by high congestion (LOS 5) the relation between travel time and flow vanishes. Non-linear regressions are illustrated for LOS 3 & 5 in Figure 7.

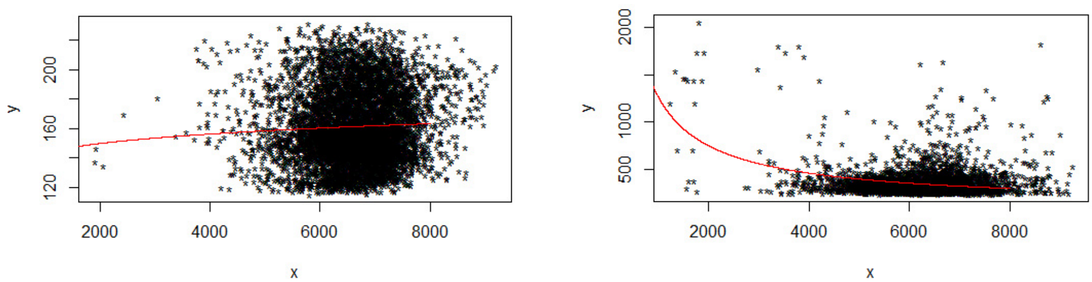

Figure 7. Non-linear regression between travel times (variable y) and flows (x) in 2002 for (a) LOS 3 (b) LOS 5

Then, applying the BPR functions on every travel time, we obtain a new “adapted” travel times series, more homogeneous, making possible a better adjustment. This happened. The improvement is very impressive for AIC values (Table 9). Due to the travel time queue, the slightest improvement is for LOS 5.The improvement remains slightly visible graphically for this LOS - see Figure 8, providing the original and adapted Singh-Maddala fits.

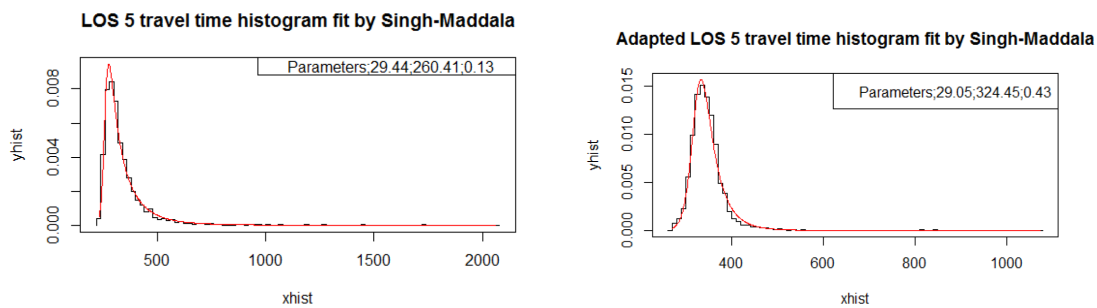

Figure 8. Histogram of original and adapted LOS 5 travel times fit by Singh-Maddala distribution in 2002

Table 9. AIC values for the five LOS travel times (originals and adapted) fit by Singh-Maddala in 2002

LOS	Number of data	Original	Adapted
1	24036	221876.36	134976
2	7878	73971.82	24642
3	6599	60821.46	20290
4	10989	101480.51	66013
5	4144	46622.16	40342

6. Conclusion and Perspectives

Basing reliability on *aggregated* travel times (here on 6-minute periods) and not on individual travel times is justified because it bases the information which is presented to users and which is taken into account in economics studies. The passage by *Levels-Of-Service* is now widespread in traffic studies because the homogeneity of a LOS induces more accurate treatments - this is confirmed here. The *Singh-Maddala* distribution is both appropriate (given the quality of the fit) and practical (for deriving percentiles, which are used in the reliability indicators). The use of BPR functions relating travel time to traffic flow (by LOS) improves the adjustments. The numerical values of the parameters vary from 2002 to 2006, likely due to a better compliance to the speed limit and to an HSR experiment in 2006. This contributes to a better understanding of travel time and of its reliability. Another study (Bhouri et al. 2014) consists in a method for identifying the impact of different factors (HSR, speed limit campaign) on the travel time distribution - however their impact on the Burr parameters is not yet performed. Further studies will identify the impacts of aggregation in time and space of the traffic data.

Acknowledgements

This work has been done with the support of Ecole des Ponts-ParisTech.

References

Al-Deek, H., Emam, E.B., 2006. New methodology for estimating reliability in transportation networks with degraded link capacities. Journal of Intelligent Transportation Systems, 117–129.

Arezoumandi, M., 2011. Estimation of Travel Time Reliability for Freeways Using Mean and Standard Deviation of Travel Time. Journal of Transp. Syst. Engineering and Info. Tech 11, 6.

Aron M., Bhouri N., Guessous Y., 2014. Estimating Travel Time Distribution for Reliability Analysis. Transport Research Arena, Paris France.

Bhouri, N., Aron, M. & Kauppila, J. , 2012. Relevance of Travel Time Reliability Indicators: A Managed Lanes Case Study Original Research. Procedia - Social and Behavioral Sciences, 54, 4 October, 450-459.

Bhouri, N., Aron, M., 2014. Isolating Different Factors Affecting Travel Time Reliability in an Observational Before/After Study, Transportation Research Procedia, 17th Meeting of the EURO Working Group on Transportation, EWGT2014,, Sevilla, Spain

Burnham, K. P., Anderson, D. R. 2004. Multimodel inference: understanding AIC and BIC in Model Selection., Sociological Methods and Research 33: 261–304 .

Heiberger, R. M., Holland, B.2004. Statistical Analysis and Data Display, Springer.

Lomax, T., Schrank, D., Tyrmer, S. & Margiotta, R., 2003. Report of Selecting Travel Reliability Measures. http://www.verkeerskunde.nl/reistijdbetrouwbaarheidsmodel Verkeerskunde. Texas Transportation Institute. Texas, USA.

Nam, D.H., Drew, D.R. 1999. Automatic measurement of traffic variables for intelligent transportation systems applications. Transp. Res. B 33, 437-457.

Pu, W., 2010. Analytic relationships between travel time reliability measures. Compendium of Papers TRB 90th Annual Meeting. Washington, D.C., USA.

Polus, A.,1979. A study of travel time and reliability on arterial routes. Transportation. 8., 141–151.

Rakha, H., El-Shawarby, I., M. Arafeh, Dion, F., 2006. Estimating Path Travel-Time Reliability. In Proceedings of the IEEE-ITSC 2006. Toronto, Canada. September 17-20.

Richardson A. J, Taylor, M.A.P., 1978. Travel time variability on commuter journeys. High Speed Ground Transportation Journal. 6. 77–79.

Singh, S.K., Maddala, G.S., 1976. A function for the size distribution of income. Econometrika 44; 963-970.

Susilawati, S., Taylor, M.A.P., Somenahalli, S.V.C., 2012. Distributions of travel time variability on urban roads. Journal of Advanced. Transportation. doi: http://dx.doi.org/10.1002/atr.192

Taylor, M, Susilawati, S., 2012. Modeling travel time reliability with the Burr distribution. Procedia - Social and Behavioral Sciences. 54. 4 October, 75–83..

Vanajakshi, D., Williams, B. M., Rilett, L. R., 2009. Improved Flow-Based Travel Time Estimation Method from Point Detector Data for Freeways. ASCE Journal of Transportation Engineering, 135, 1. 26-36.